Available online at www.sciencedirect.com

ScienceDirect

Procedia Technology 22 (2016) 501 – 508

Procedia Technology

9th International ConferenceInterdisciplinarity in Engineering, INTER-ENG 2015, 8-9 October 2015, TirguMures, Romania

An Efficiency PI Speed Controller for Future Electric Vehicle in Several Topology

Brahim Gasbaoui[a,]*, Abdelfatah Nasri[a],Othmane Abdelkhalek[a]

[a]*Laboratory of Smart Grids & Renewable Energies (S.G.R.E.).Faculty of technology, Department of Electrical Engineering, Bechar University B.P 417 (08000), Algeria*

Abstract

In this paper a four-Wheels-Drive (4WD) Electric Vehicle (EV) controlled by Direct Torque Control (DTC) is presented, where neural network PI speed controller is proposed to tune the PI controller gains to ensure optimal performance of 4WD Electric Vehicle. The electrical traction chain was well analyzed and studied from the Lithium Ion (Li-Ion) battery, the buck boost to the mechanical load behavior. The speed of the four wheels is calculated independently during the turning with the electronic differential system computations which distributes torque and power to each in-wheel motor according to the requirements, adapts the speed of each motor to the driving conditions. The basic idea of this work is to maintain the initial battery state of charge (SOC) equal to 60% and the prototype was tested in several topology conditions and under speed. Our electric vehicle direct torque control is simulated in MATLAB SIMULINK environment. 4WD Electric vehicle (EV) has demonstrated satisfactory results in all kind of roads constraints: straight, ramp, curved road and downhill. The analysis and simulations lead to the conclusion that the proposed system is feasible. Results also indicate that this strategy can be successfully implemented into the traction drive of the modern 4WD electric vehicles.

Peer-review under responsibility of the "Petru Maior" University of Tirgu Mures, Faculty of Engineering

*Keywords:*Neural Networks; PI speed control; DTC, Electric vehicle; SOC.

1. Introduction

The principal constraints in vehicle design for transportation are the development of a non-polluting high safety

* Corresponding author. Tel.: +213556692800; fax: +213040854557.
*E-mail address:gasbaoui_2009@*yahoo.com

Peer-review under responsibility of the "Petru Maior" University of Tirgu Mures, Faculty of Engineering
doi:10.1016/j.protcy.2016.01.109

and comfortable vehicle. Taking into account these constraints, our interest has been focused on the 4WD electric vehicle, with independent driving wheel-motor at the front and with classical motors on the rear drive shaft [1, 2, 3, 4].This configuration is a conceivable solution, the pollution of this vehicle is strongly decreased and electric traction gives the possibility to achieve accurate and quick control of the distribution torque. Torque control can be ensured by the inverter, so this vehicle does not require a mechanical differential gear or gearbox. One of the main issues in the design of this vehicle (without mechanical differential) is to assume the stability. During normal driving condition, all drive wheel system requires a symmetrical distribution of torque in the both sides. In recent years, due to problems like the energy crisis and environmental pollution, the Electric Vehicle (EV) has been researched and developed more and more extensively [1,2].

Currently, most EV is driven by two front wheels or two rear wheels. Considering some efficiency and space restrictions on the vehicle, people have paid more and more attention in recent years to four-wheel drive vehicles employing the IM in-wheel motor. The Direct Torque Control strategy (DTC) is one kind of high performance driving technologies for AC motors, due to its simple structure and ability to achieve fast response of flux and torque has attracted growing interest in the recent years. The main advantages of DTC are robust and fast torque response, no requirements for PWM pulse generation and current regulators, as well as good steady-state and dynamic performances. The DC-DC converter is used with a wide range in electric vehicles to assure the energy require for the propulsion system.

This paper proposes a neural network PI speed control approach of an electrical differential system for an EV propelled by four induction motor drives (one for each wheel) [8].Indeed, neural network concepts have become an active research area in power electronics and motor drives. Because of the necessity for adaptive abilities in a network learning process, applying neural networks to system identification and control dynamics has become a promising alternative to process control. Neural networks can be applied to control and identify nonlinear systems since they approximate any desired degree of accuracy with a wide range of nonlinear models [9, 10,7].

The aim of this paper is to understand the lithium-ion battery comportment controlled by DC-DC converter, each wheels is controlled independently by using direct torque control based space vector modulation under several topology and speed variation. Modeling and simulation are approved out using the Matlab/Simulink tool to study the performance of 4WD proposed system.

Nomenclatures

4WD	Four-Wheels-Drive
EV	Electric Vehicle
DTC	Direct Torque Control
PM	Positive Medium
SOC	Stat of charge
PWM	Plush width modulation
Li-Ion	Lithium Ion
DC	Direct Current
IM	Induction Motor
PI	Proportional and Integral

2. Electric Vehicle description

According to Figure 1 the opposition forces acting to the vehicle motion are: the rolling resistance force F_{tire} due to the friction of the vehicle tires on the road; the aerodynamic drag force F_{aero} caused by the friction on the body moving through the air, and the climbing force F_{slope} that depends on the road slope [1, 2, and 3].

The total resistive force is equal to F_r and is the sum of the resistance forces:

$$F_r = F_{tire} + F_{aero} + F_{slope} \quad (1)$$

The rolling resistance force is defined by:

$$F_{tire} = mgf_r. \quad (2)$$

The aerodynamic resistance torque is defined as follows:

$$F_{aero} = \frac{1}{2}\rho_{air} A_f C_d v^2 \quad (3)$$

The rolling resistance force is usually modelled as:

$$F_{slope} = mg\sin(\beta) \quad (4)$$

where r is the tire radius, m is the vehicle total mass, f_r is the rolling resistance force constant, g the gravity acceleration, ρ_{air} is air density , C_d is the aerodynamic drag coefficient, A_f is the frontal surface area of the vehicle, v is the vehicle speed, β is the road slope angle. Values for these parameters are shown in Table1.

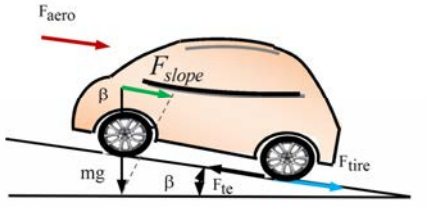

Fig. 1.The forces acting on a vehicle moving along a slope.

Table 1. Parameters of the electric vehicle model.

r	A_f	m	C_d	f_r	ρ_{air}
0.32 m	2.60 m^2	1300 Kg	0.32	0.01	1.2 Kg/m^3

3. Direct torque control strategy

The basic DTC strategy is developed in 1986 by Takahashi. It is based on the determination of instantaneous space vectors in each sampling period regarding desired flux and torque references. The reference speed is compared to the measured one [11]. The obtained error is applied to the speed regulator PI whose output provides the reference torque. The estimated stator flux and torque are compared to the corresponding references. The errors are applied to the stator flux and torque hysteresis regulators, respectively:

$$\phi_{\alpha s} = \int_0^t (V_{\alpha s} - R_s i_{\alpha s})dt \quad (5)$$

$$\phi_{\beta s} = \int_0^t (V_{\beta s} - R_s i_{\beta s})dt \quad (6)$$

$$|\phi_s| = \sqrt{\phi_{\alpha s}^2 + \phi_{\beta s}^2} \quad (7)$$

$$\phi_s = \tan^{-1}\left(\frac{\phi_{\beta s}}{\phi_{\alpha s}}\right) \quad (8)$$

And electromagnetic torque T_{em} can be calculated by:

$$T_{em} = \frac{3}{2} p(\phi_{\alpha s} i_{\beta s} - \phi_{\beta s} i_{\alpha s}) \quad (9)$$

Where ϕs is the is the stator flux , $\phi_{\alpha s}$ and $\phi_{\beta s}$ are the stator flux in $\alpha\beta$ components , R_s is the stator resistance, T_{em} is the electromagnetic torque , $V_{\alpha s}$ and $V_{\beta s}$ are the stator voltages in $\alpha\beta$ components , $i_{\alpha s}$ and $i_{\beta s}$ are the stator currents in $\alpha\beta$ components.

4. Simulation results

In order to characterize the driving wheel system behavior, simulations were carried using the model of Figure2. The following results were simulated in MATLAB and its divided in two phases. The first one deal with the test of the EV performances controlled with DTC strategy under several speed variations in the other hand we show the

impact of this controller on vehicle performance power electronics. Only the right motor simulations are shown. The assumption is that the initialized Li-Ion battery SOC is equal to 60%.

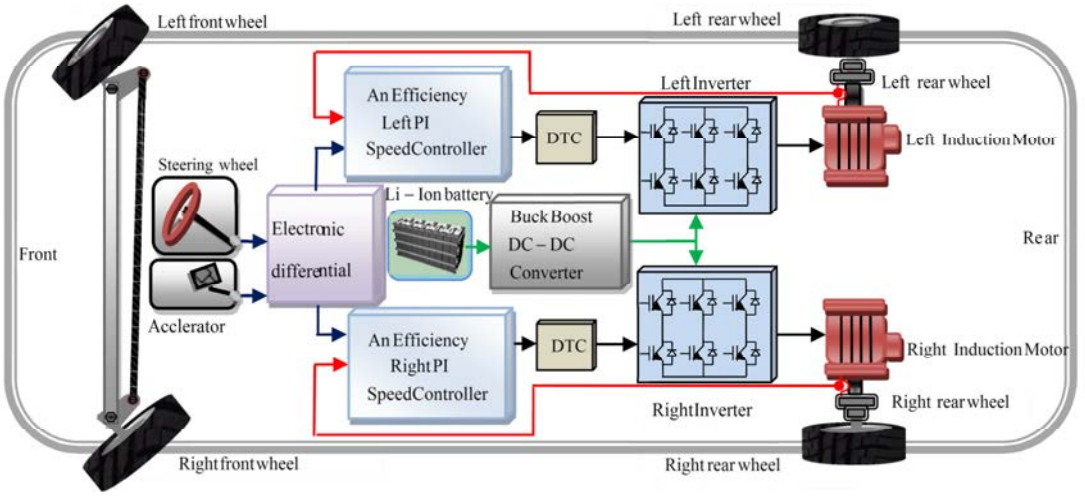

Fig. 2. The driving wheels control system.

A: Direct torque control scheme

The topology studied in this work consists of three phases: the first one represent the acceleration phase's beginning with 60 Km/h in straight road, the second phase represent the deceleration one when the speed became 30Km/h, and finally the EV is moving up the slopped road of 10% under 80 Km/h, the specified road topology is shown in Figure3, when the speed road constraints are described in the Table 2.

Table 2. Specified driving route topology.

Phases	Event information	Vehicle Speed[Km/h]
Phase 1	Acceleration	60
Phase 2	Bridge, Break	30
Phase 3	Acceleration and climbing a slope 10%	80

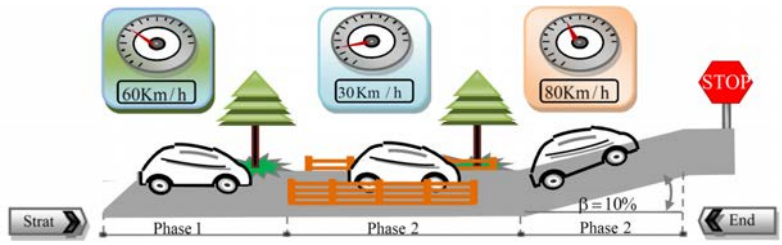

Fig.3. Specify driving route topology.

Refereed to Figure 4 at time of 2 s the vehicle driver move on straight road with linear speed of 60 Km/h, the assumption's that the two motors are not disturbed and the initial state of charge of 60 % is respected.

Figures 5 and 6 explain the variation of phase current and driving force respectively. In the first step and to reach 60 Km/h the EV demand a current of 50.69 A for each motor which explained with driving force of 329.28 N. In second phase the current and driving forces demand decrees by means that the vehicle is in recharging phase's which explained with the decreasing of current demand and developed driving forces shown in Figures 5 and 6 respectively. The last phases explain the effect of acceleration under the slope on the straight road EV moving.

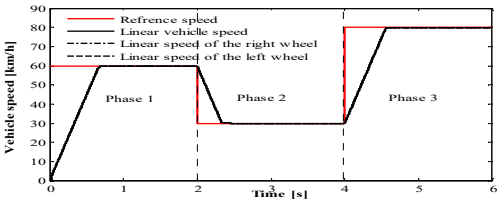

Fig.4. Variation of vehicle speeds in different scenarios.

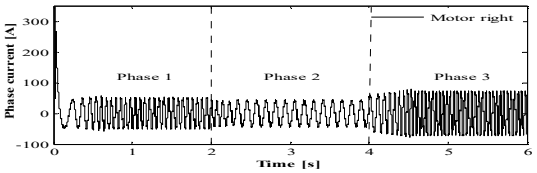

Fig.5. Variation of phase current of the right motor in different phases.

The driving wheels forces increase and the current demand undergo double of the current braking phases the battery use 80 % of his power to satisfy the motorization demand under the slopped road condition which can interpreted physically the augmentation of the globally vehicle resistive. In the other hand the linear speeds of the two induction motors stay the same and the road drop does not influence the torque control of each wheels. The results are listed in Table 3.

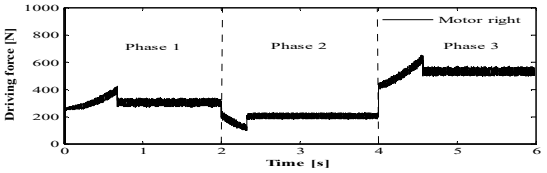

Fig.6. Variation of driving force of the right motor in different phases.

According to the formulas (1), the variation of resistive vehicle torques in different cases is depicted in Table 4. The vehicle resistive torque was 95.30 Nm in the first case (acceleration phase) when the power propulsion system resistive one is only 68.51 Nm in the breaking phases (phases 2), the back driving wheels develop more and more efforts to satisfy the traction chain demand which impose an resistive torque equal to 167.99 Nm. The result prove that the traction chain under acceleration demand develop the double effort comparing with the breaking phase case's by means that the vehicle needs the half of its energy in the deceleration phase's compared with the acceleration one's as it is specified in Table 4.

Table 3. Values of phase current driving force of the right motor in different phases.

Phases	Phase 1	Phase 2	Phase 3
Current of the right motor [A]	50.69	44.20	70.77
Driving force of the right motor [N]	329.28	228.48	562.00

Table 4. Variation of vehicle torque in different Phases.

Phases	1	2	3
Vehicle resistive torque [N.m]	95.30	68.51	167.99
Globally vehicle resistive torque Percent compared with nominal motor torque of 476 Nm [%]	20.01	14.38	35.20

B: Power electronics

The Lithium Ion must be able to supply sufficient power to the EV in accelerating and decelerating phase, which means that the peak power of the batteries supply must be greater than or at least equal to the peak power of the both electric motors. The battery must store sufficient energy to maintain their SOC at a reasonable level during driving, the Fig.7 (a) ,7(b),7(c) and 7(d) describes the changes vehicle speed ,globally motor torque , battery current, and state of charge in different scenarios.

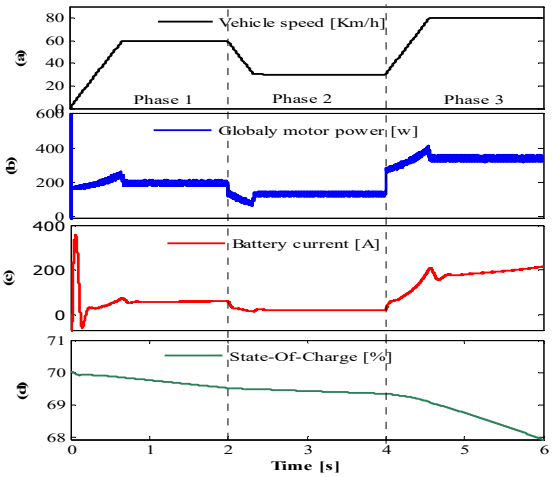

Fig.7. Variation of parameters during consideration scenario (a) vehicle speed; (b) globally motor power; (c) battery current; (d) SOC

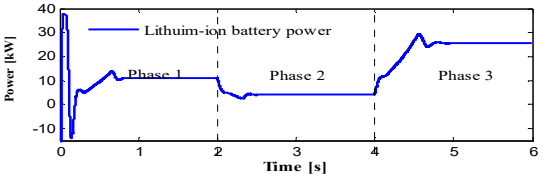

Fig. 8. Variation of Li-Ion battery power in different phases.

Table 5. Values of Li-Ion battery power in different phases.

Phase	Phase 1	Phase 2	Phase 3
Battery power [kW]	10.06	4.11	25.59
Percentage of the battery power compared with globally motor power [%]	32.46	13.27	82.56

Table 5 and describe the power distribution in the electrical traction under several speed references. The used battery produced power depend only on the electronic differential consign by means the acceleration/deceleration driver state which can be explained by the battery SOC of Figure 7(b) [5].

In Figure 8, the battery provides about 10.06 Kw in the first phase in order to reach the electronic differential reference speed of 60 Km/h. In the second phase (phase 2: deceleration phase's) the demanded power battery decreased about 5.95 Kw that present 71.91% of the globally nominal power battery (31 Kw). In third phase the battery produced power is equal to 25.59 Kw under slopped road state the Table. 6 give evaluation of SOC [%] in the different phases.

Table 6. Evaluation of SOC [%] in the different phases.

Phase	Speed [Km/h]	Begin Phase [s]	End Phase[s]	SOC begin	SOC end	SOC diff
1	60	0	2	60.00	59.50	0.5
2	30	2	4	59.50	59.32	0.18
3	80	4	6	59.32	57.80	1.52

Fig. 9 explains how SOC in the Li-Ion battery changes during the driving cycle; it seems that the SOC decreases rapidly at acceleration, by means that the SOC range's between 57.81% to 60% during all cycle's phases from beginning at the end cycles. At t = 6 s, the battery SOC becomes lower than 57.82 % (it was initialized to 60 % at the beginning of the simulation).The final state of charge are 57.81 %.

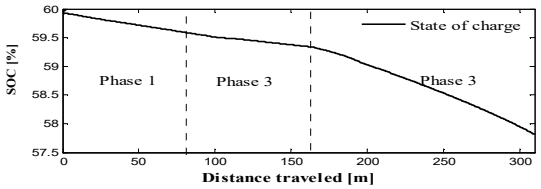

Fig.9. Variations of the SOC during travelled distance in versus vehicle speed.

Figure 9 and Table 7 investigate the variation of sate of charge during travelled distance respectively. The relationship between SOC and left time in three phases are defined by the flowing linear fitting formula:

$$SOC[\%] = 0.0010147t^6 - 0.014954t^5 + 0.072173t^4 - 0.12693t^3 + 0.058746^2 t + -0.1674t + 59.978 \quad (10)$$

Moreover the simulation results specified by Figure 9, we can define the relationship between the sate of charge and the traveled distance in each cases, the first one (acceleration) is defined by the linear fitting formula:

$$SOC[\%] = -0.006 d_{traveled} + 60 \quad (11)$$

The second (deceleration) is obtained and represented by:

$$SOC[\%] = -0.0020 d_{traveled} + 59.67 \quad (12)$$

Finally the third phase's formula (acceleration under slope) is given by:

$$SOC[\%] = -0.01 d_{traveled} + 60.98 \quad (13)$$

Table 7. Evaluation of distance traveled and SOC

Phases	Distance traveled [m]	SOC Difference [%]	P consumed [Kw]
Phase 1	81.57	0.5	10.07
Phase 2	82.63	0.18	4.12
Phase 3	145.80	1.52	25.60

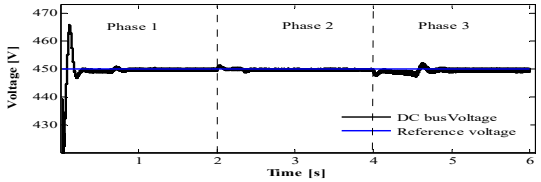

Fig. 10. Robustness test of Buck Boost DC-DC converter under several speed variations.

This power is controlled by the Buck Boost DC-DC converter current and distribute accurately for three phases [6]. From Figure10 we test the buck boost DC-DC converter robustness under several speed cycles. When the speed passes from 30 Km/h to80 Km/h, the demanded voltage is 450 V. The buck boost converter is not only a robust converter which ensures the power voltage transmission but also a good battery recharger in deceleration state that help to perfect the vehicle autonomous with no voltage ripple. Table 8 gives voltage ripple in different cases in electrical traction system when the ripple rate changes are affected with the phase's states.

Table 8. Evaluation of voltage ripple.

Phases	1	2	3
The voltage ripple [V] [%]	0.93	0.55	1.0

C: Case of an Efficiency PI speed controller

To compare the effect of disturbances on the vehicle speed in the cases of two types of control, Table 9, shows the system response in two cases Neural network PI speed control and PI classical control [12,13]. We can say that: the effect of the disturbance is neglected in the case intelligent PI speed control.

It appears clearly that the classical control with PI controller is easy to apply. However, the control with the genetic algorithm controllers offers better performances in both of the overshoot control and the tracking error. In

addition to these dynamic performances, it respects the imposed constraints by the driving system such as the robustness of parameter variations. Table 10 proves that the intelligent Neural network PI speed control minimize the aerodynamic torque leading to the decrease of the front section of the electric vehicle and augmentation of autonomy battery power.

Table 9. Performances of the Neural network PI speed control in the speed response.

Parameter and indexes	PI classical	An Efficiency PI speed controller
Overshoot [%]	0.5500	0.0107
Rise time (sec)	0.7077	0.21
Steady state error [%]	1.0182e+001	6.8542e+000

Table 10. Comparative Study.

Parameter and indexes	PI speed control	An Efficiency PI speed controller
Aerodynamic torque [Nm]	50.08	49.47
Vehicle torque [Nm]	88.98	88.07
Current [A]	54.93	54.00
Electromagnetic torque [Nm]	126.50	125.09

5. Conclusion

In this paper, An Efficiency PI speed controller based neural network is designed and simulated to increase the electric vehicle performance. The power propulsion system studied in this paper has demonstrated that the Lithium Ion battery behaviour controlled by buck boost DC-DC converter for utility EV which utilize tow rear deriving wheel for motion can be improved using direct torque control strategy based on space vector modulation when the battery developed power depend on the speed reference of the driver. The several speed variations do not affect the performances of the Lithium Ion battery and the control strategy gives good dynamic characteristics of the EV propulsion system. This paper proposes novel fitting formulas which give the relationship between the SOC and distance travelled and others formulas that give more efficiency to different propulsion systems paths.

Acknowledgements

The authors would like to acknowledge the Laboratory of Smart Grids and Renewable Energies (S.G.R.E.) from Bechar (Algeria) University.

References

[1] Salman M, Chang M, Chen J. Predictive energy management strategies for hybrid vehicles. IEEE VPPC, Chicago, IL 2005;21–25.
[2] Larminie J, Lowry J. Electric Vehicle Technology Explained. Edited by John Wiley and John Lowry, England; 2003.
[3] Nelson RF. Power requirements for battery in HEVs. J. Power Sources 2000; 91:2–26.
[4] Xia C, Guo Y. Implementation of a Bi-directional DC/DC Converter in the Electric Vehicle. J of Power Electronics 2006;40(1):70–72.
[5] Ramadass P, et al. Capacity fade of Sony 18650 cells cycled at elevated temperatures: Part IL Capacity fade analysis. Journal of Power Sources 2002;112:614 - 620.
[6] Zhang YY. Analysis and Evaluation of Bidirectional DC/DC Converter. Journal of Power Technology 2003;1(4):331–338.
[7] Gupta AK, Khambadkone AM. A general space vector PWM algorithm for multilevel inverters, including operation in overmodulation range, IEEE Trans. Power Electron. 2007:22(2):517–526.
[8] Yan XX, Patterson D. Novel power management for high performance and cost reduction in an electric vehicle. Renew. Energy 2001;22(1–3):177–183.
[9] Chill HJ, Lin LW. A Bidirectional DC-DC Converter for Fuel Cell Electric Vehicle Driving System. IEEE Trans. Power Electron 2006; 21: 950–958.
[10] Nasri A, Bousserhane IK, Hadjeri S, Sicard P. Fuzzy logic Speed control stability improvement of lightweight electric vehicle drive. Journal of electrical engineering b & Technology 2010;5(1):129~139.
[11] Habetler TG, Profumo F, Pastorelli M, Tolbert L. Direct torque control of induction machines using space vector modulation. IEEE Transaction on Industry Applications 1992;28(5):1045-1053.
[12] Moldovan L. Geometrical Method for Description of the 6-PGK Parallel Robot's Workspace. Complexity in Artificial and Natural Systems Proceedings 2008;23-30.
[13] Moldovan L. Trajectory Errors of the 6-PGK Parallel Robot. Complexity in Artificial and Natural Systems Proceedings 2008;68-75.